viruses

MDPI

Article

Roles of the Endogenous Lunapark Protein during Flavivirus Replication

Pham-Tue-Hung Tran, Naveed Asghar, Magnus Johansson *,† and Wessam Melik *,†

Inflammatory Response and Infection Susceptibility Centre (iRiSC), School of Medical Science, Örebro University, 703 62 Örebro, Sweden; hung.tran@oru.se (P.-T.-H.T.); naveed.asghar@oru.se (N.A.)

* Correspondence: Magnus.Johansson@oru.se (M.J.); Wessam.Melik@oru.se (W.M.)

† These authors contributed equally to this work.

Abstract: The endoplasmic reticulum (ER) of eukaryotic cells is a dynamic organelle, which undergoes continuous remodeling. At the three-way tubular junctions of the ER, the lunapark (LNP) protein acts as a membrane remodeling factor to stabilize these highly curved membrane junctions. In addition, during flavivirus infection, the ER membrane is invaginated to form vesicles (Ve) for virus replication. Thus, LNP may have roles in the generation or maintenance of the Ve during flavivirus infection. In this study, our aim was to characterize the functions of LNP during flavivirus infection and investigate the underlying mechanisms of these functions. To specifically study virus replication, we generated cell lines expressing replicons of West Nile virus (Kunjin strain) or Langat virus. By using these replicon platforms and electron microscopy, we showed that depletion of LNP resulted in reduced virus replication, which is due to its role in the generation of the Ve. By using biochemical assays and high-resolution microscopy, we found that LNP is recruited to the Ve and the protein interacts with the nonstructural protein (NS) 4B. Therefore, these data shed new light on the interactions between flavivirus and host factors during viral replication.

Keywords: flavivirus; Kunjin virus (WNV_{KUN}); Langat virus (LGTV); Zika virus (ZIKV); replication; replicon-expressing cell line; lunapark (LNP); NS4B

Citation: Tran, P.-T.-H.; Asghar, N.; Johansson, M.; Melik, W. Roles of the Endogenous Lunapark Protein during Flavivirus Replication. *Viruses* **2021**, *13*, 1198. https://doi.org/10.3390/v13071198

Academic Editors: Daniela Ribeiro and Markus Islinger

Received: 27 April 2021
Accepted: 17 June 2021
Published: 22 June 2021

1. Introduction

The genus *Flavivirus* (family *Flaviviridae*) consists of important zoonotic viruses causing morbidity and mortality worldwide. Within the genus, the mosquito-borne neurotropic West Nile virus (WNV) may cause severe meningoencephalitis [1]. Similarly, Zika virus (ZIKV) is another mosquito-borne flavivirus, which has gained public attention by causing congenital microcephaly or Guillain–Barré syndrome at recent outbreaks in 2014–2015 [2]. In addition, there are also tick-borne flaviviruses causing neurotropic diseases. Among them, infection with tick-borne encephalitis virus (TBEV) Far-Eastern subtype may result in severe encephalitis with mortality rates as high as 20–30% in Eurasia [3,4].

Flaviviruses are enveloped, single-stranded positive-sense RNA viruses with an icosahedral structure. The viral genome is about 11 kb with one open reading frame (ORF) encoding a polyprotein. Cleavages of the polyprotein by host and viral proteases at the endoplasmic reticulum (ER) membrane result in three structural proteins: capsid (C), precursor membrane (prM), envelope (E); and seven non-structural proteins (NS; NS1 to NS5). The viral genome also contains two untranslated regions (UTRs) flanking the ORF [5].

During flavivirus infection, the ER membrane invaginates into the luminal side, forming packets of bilayer membrane vesicles (Ve), where the replication complex (RC) of NS proteins and the viral RNA are located [5–7]. The viruses replicate their RNA genome at the generated Ve, followed by genome encapsidation and envelopment. New particles transit from the ER to the Golgi, followed by a particle maturation process at the trans-

Golgi network. Ultimately, the newly formed viruses are released from infected cells by exocytosis.

At the Ve, NS2A, NS2B, NS4A, and NS4B are transmembrane (TM) proteins, acting as scaffolds for the RC. Overexpression of NS4A or NS4B can trigger the ER membrane invagination, which results in vesicles morphologically similar to the Ve [8–10]. Before cleavage of the polyprotein, NS4A and NS4B are bridged by a conserved 23-amino-acid-long signal peptide with a molecular weight of 2,000 Da (2K). The two proteins are cleaved by the viral protease NS2B/NS3 and a host peptidase [8].

In eukaryotic cells, the ER is a large membrane-based organelle that spreads throughout the cytoplasm presenting three major morphologies: the nuclear envelope, the peripheral ER cisternae, and the interconnected tubular network [11]. To induce and maintain the highly curved tubular structure, host machinery is employed, including the reticulon (RTN) family of integral membrane proteins, the DP1/Yop1 proteins [12,13], the atlastin (ATL) family of dynamin-like GTPases [14,15], and the lunapark (LNP) protein [16,17]. Due to their membrane-remodeling capacities and the location within ER, these host proteins may have roles in flavivirus replication and the formation of the Ve. It has previously been shown that silencing of RTN3.1A [18], ATL2, or ATL3 [19,20] resulted in reductions of flavivirus titers. However, the putative roles of the other ER membrane-shaping proteins, such as LNP, remains to be clarified during flavivirus infection.

In this study, we aimed to characterize the functions of the host LNP during flavivirus infection. We used the Kunjin strain of WNV ($WNV_{KUN)}$ and ZIKV strain SL1602 Suriname 2016, as mosquito-borne flavivirus models. In addition, we used Langat virus strain TP21 (LGTV), which belongs to the TBEV serocomplex [3,21], as the tick-borne flavivirus model. We generated cell lines expressing the WNV_{KUN} and LGTV replicons to study the role of LNP during virus replication. We found that the LNP protein is essential for virus replication and maintenance of the Ve. Conclusively, we demonstrate that the flavivirus NS4B recruits LNP to the Ve at its C-terminus, which suggests a role for LNP within the underlying mechanism of Ve generation.

2. Materials and Methods

2.1. Cell Culture

Baby hamster kidney (BHK-21), Vero B4, human embryonic kidney 293 (HEK293), and A549 cells were maintained in Dulbecco's Modified Eagle's Medium (DMEM) containing 1 g/L glucose (Gibco, Paisley, UK) supplemented with 10% heat-inactivated fetal bovine serum (HI-FBS) (Gibco), 100 U/mL penicillin–streptomycin (PEST) (Gibco), and 1% nonessential amino acids (NEAA) (Gibco) at 37 °C in 5% CO_2.

2.2. Viruses

An infectious clone of WNV_{KUN} based on FLSDX sequence (accession number AY274504) was rescued. In short, the sequences were chemically synthesized and cloned into DNA vectors to generate two constructs: pKUNV-CME and pKUNV-luc-rep. pKUNV-CME comprises an SP6 promoter sequence and the 5′NCR, the structural genes, and 668 bp of NS1 of WNV_{KUN}, whereas pKUNV-luc-rep is an established KUNV replicon where most of the structural cassette is replaced with firefly luciferase reporter gene as described previously [3]. The plasmids were cleaved by suitable restriction enzymes and ligated to generate a pSP6-KUNV construct with an SP6 promoter upstream the 5′-UTR and the hepatitis delta virus ribozyme (HDVr) sequence immediately downstream of the 3′-UTR of the complete KUNV sequence. The cloning work was performed using standard molecular biology procedures and verified by DNA sequencing (Eurofins MWG Operon, Germany). The pSP6-KUNV construct was linearized prior to RNA synthesis followed by capping to generate a complete WNV_{KUN} RNA genome, using MEGAscript SP6 in vitro transcription kit (Ambion, USA) as per the manufacturer's instructions. The capped RNA-transcripts were transfected into a mixed (1:1) population of HEK293 and Vero B4 cells to rescue the infectious virus as described previously [22]. LGTV strain TP21 was a kind gift from A. K.

Överby (Department of Clinical Microbiology, Virology, Umea University, Sweden). ZIKV strain SL1602 (accession number KY348640) originated from Suriname was obtained from the European Virus Archive.

2.3. Preparation of Gene Constructs

The WNV_{KUN} replicon was constructed based on the WNV_{KUN} sequence (accession number AY274504), as described previously [3]. Briefly, the replicon is driven by a T7 promoter expressing an ORF of WNV_{KUN} where most of the structural cassette is replaced with firefly luciferase reporter gene (*Luc*). The foot-and-mouth disease virus autoprotease 2a sequence was fused in frame after *Luc* for post-translational cleavage release of the reporter. The ORF is flanked by the 5′-UTR and the 3′-UTR and a hepatitis delta virus antigenomic ribozyme sequence is inserted immediately downstream of the WNV_{KUN} 3′-UTR followed by the Simian virus 40 polyadenylation signal. An IRES sequence and a NeoR/KanR gene which confers G418 antibiotic resistance was inserted into the 3′-UTR sequence. The LGTV replicon was constructed similarly, and its sequence is based on the LGTV strain TP21 (accession number NC003690).

The TBEV Torö-2003 strain (accession number AH013799) was used as a template to clone NS4A-NS4B, NS4A, 2K-NS4B, 2K-NS4B TM1-3, 2K-NS4B TM1, anchor-prM-E genes into the plasmid pmCherry (Clonetech) introducing a C-terminal mCherry tag to the proteins.

pHAGE2 Lnp-mCherry was a gift from Tom Rapoport (Addgene plasmid # 86687; http://n2t.net/addgene:86687; accessed on 18 June 2021; RRID:Addgene_86687) [23].

2.4. Establishment of Cell Line Expressing RNA WNV_{KUN} or LGTV Replicons

The WNV_{KUN} or LGTV DNA-based replicon construct was linearized by ClaI enzyme, followed by in vitro transcription and cap analog incorporation using mMESSAGE mMACHINE™ T7 Transcription Kit (Invitrogen, Vilnius, Lithuania). The RNA was purified using RNeasy Mini Kit (Qiagen, Hilden, Germany) prior to transfection into BHK-21 cells by Lipofectamine™ MessengerMAX™ Transfection Reagent (Invitrogen). Two days after transfection, the cell culture was supplemented with 600 µg/mL G418 (Invivogen, Toulouse, France) to select transfected cells.

2.5. Transfection

70% confluent A549 cells in a 24-well plate were incubated with a premix of 100 µL OptiMEM medium (Gibco), 10 pmol siRNAs against LNP (Catalogue number: L-023148-01-0005, Horizon Discovery, Cambridge, UK) or non-targeting (NT) siRNA (Catalogue number: D-001810-01-20, Horizon Discovery, UK), and 1 µL of lipofectamine RNAiMAX reagent (Invitrogen) for 24 h, according to the manufacturer's instructions. For BHK-21 replicon stable cell lines, the treatment was repeated twice.

50–100 ng of the LNP-mCherry construct was transfected in A549 cells grown in 24 well-plates, using Lipofectamine 2000 (Invitrogen).

2.6. Virus Infections and Cell Harvesting

After transfections for 24 h, A549 cells were infected by WNV_{KUN}, ZIKV, or LGTV with 0.1 multiplicity of infection. Supernatants were harvested 24 h post-infection and cells were detached by trypsin, followed by a soybean trypsin inhibitor treatment (Gibco). Cells were then briefly frozen in liquid nitrogen and thawed repeatedly three times.

2.7. Antibodies

The following antibodies were used in this study: rabbit anti-LNP (Atlas Antibody, Stockholm, Sweden), monoclonal mouse-LGTV E (clone 11H12, United States Army Medical Research, Institute of Infectious Diseases, Fort Detrick, Frederick, MD, USA), mouse anti-mCherry tag (Novus Biologicals, Englewood, CO, USA), rabbit anti-mCherry tag (Novus Biologicals, USA), mouse anti-GAPDH (Sigma, St. Louis, MO, USA), Alexa Fluor

594-conjugated anti-mouse goat antibody (Invitrogen), Alexa Fluor 488-conjugated anti-rabbit goat antibody (Invitrogen), anti-mouse VisUCyte HRP Polymer (R&D Systems, Minneapolis, MN, USA) and HPR-conjugated anti-mouse goat antibody (Invitrogen).

2.8. Plaque Assays

Crystal violet-based plaque assays were performed to quantify infectious WNV_{KUN} and ZIKV particles, while immuno-focus plaque assays were performed to quantify infectious LGTV. In brief, series of virus dilutions in DMEM were used to infect 90% confluent Vero cells for 1 h at 37 °C, followed by cell-overlaying with DMEM supplemented with 1.2% Avicel (FMC, Philadelphia, PA, USA), 2% HI-FBS, 1X NEAA, 1% PEST. After 3–4 days, the overlays were removed, and cells were fixed with methanol for 20 min before performing plaque assays. For immuno-focus assay, the fixed cells were blocked by 2% BSA for 10 min before being labeled with 1:1000 mouse LGTV E, then 1:100 VisUCyte anti-mouse secondary HRP Polymer for 1 h at 37 °C, respectively. Finally, the cells were incubated with KPL TrueBlue Peroxidase Substrate (Seracare, Milford, MA, USA) for 20 min at room temperature (RT). For crystal violet-based plaque assay, the fixed cells were stained with 1% crystal violet (Sigma), 20% methanol (Fisher, Trinidad and Tobago), and 1% ammonium oxalate (Sigma) solution.

2.9. Quantitative Real-Time PCR (qPCR)

Total RNA was isolated from cell lysates or cell culture supernatants using RNeasy Mini kit (Qiagen) or QIAamp Viral RNA Mini Kit (Qiagen), respectively. cDNA was synthesized using a High-Capacity cDNA Reverse Transcription kit (Applied Biosystems, Vilnius, Lithuania) with specific primers targeting the WNV_{KUN}, ZIKV, or LGTV positive strand (Table 1). qPCR was conducted using a QuantStudio 7 Flex Real-Time PCR System (Applied Biosystems) with TaqMan Fast Advanced Master Mix (Applied Biosystems) and Custom TaqMan Gene Expression Assays (Applied Biosystems) containing specific primers and probes (Table 1).

Table 1. List of primers and probes used for qPCR.

Assay	Virus	Sequence (5′–3′)
cDNA synthesis	WNV_{KUN}	AATATGCTGTGTTGTTGTGG
	ZIKV	GATCTTGGTGAATGTGAACG
	LGTV	CTCCCTGTGAGTTCATAATTGG
qPCR assay	WNV_{KUN}	CAGACCACGCCATGGCG
		CTAGGGCCGCGTGGG
		FAM-TCTGCGGAGAGTGCAGTCTGCGA-NFQ
	ZIKV	CCGCTGCCCAACACAAG
		CCACTAACGTTCTTTTGCAGACAT
		FAM-AGCCTACCTTGACAAGCAGTCAGACACTCAA-NFQ
	LGTV	ACTGAACTGGAGAAGGAGGA
		CCACAGTCCCATGACGATAAG
		FAM-TAGGCTTGATTGCCTCGGCCTTTC-NFQ

2.10. Luciferase Assay

Cell lysates were assayed for bioluminescence using Dual-Luciferase Reporter Assay kit (Promega, USA) at a Lumi-star Omega (BMG Labtech, Ortenberg, Germany), according to the manufacturer's instructions.

2.11. Protein Electrophoresis and Immunoblotting

Cells were lysed by 0.5% SDS prior to boiling in 1X LDS sample buffer (Invitrogen). Proteins were separated on precast 4–12% polyacrylamide Bis-Tris gels (Invitrogen) in MES running buffer (Invitrogen) for 60 min at 120 V constant before being transferred to nitrocellulose membranes using iBlot 2 Gel Transfer Device (Invitrogen). Proteins of interest were detected with the antibodies anti-mCherry (1:1000), anti-LNP (1:1000), and anti-GAPDH (1:2000).

2.12. Immunoprecipitations (IP)

For protein-protein interaction studies, A549 cells were transfected with the gene constructs using a NucleofectorTM 2b Device (Lonza, Basel, Switzerland) and Cell Line NucleofectorTM Kit T (Lonza). Two days post-transfection, the cells were lysed by radioimmunoprecipitation assay (RIPA) buffer (Sigma) supplemented with a protease inhibitor cocktail (Sigma) for 20 min at 4 °C. Lysates were pre-cleared by centrifuge at 1000× *g* for 10 min. 300 µg of the pre-cleared lysates were incubated with 4 µg of mouse anti-mCherry, 50 µL of a protein G-tagged microbead pre-mix (MACS, Stockholm, Sweden) at 4 °C for 1 h. The mixtures were then loaded on µ Columns (MACS) holding on a µMACS Separator to retain the microbeads on the columns. The beads were washed four times with 4 °C 50% RIPA buffer. Finally, bead-binding proteins were eluted by a pre-heated 95 °C LDS sample buffer.

2.13. Transmission Electron Microscopy (TEM)

Cells were fixed in 2.5% glutaraldehyde (Ladd, Bureau County, IL, USA) in 0.1 M phosphate buffer pH 7.4 at RT for 1 h, followed by storage at 4 °C. Following the primary fixation, the cells were rinsed with 0.1 M phosphate buffer and post-fixed in 2% osmium tetroxide in 0.1 M phosphate buffer, pH 7.4 at 4 °C for 2 h. The cells were then ethanol dehydrated stepwise, followed by stepwise acetone/LX-112 infiltration, and finally embedded in LX-112 (Ladd). Semi-ultrathin sections were prepared using the EM UC 7 (Leica, Wetzlar, Germany). The ultrathin sections (approximately 60–80 nm) were contrasted with uranyl acetate followed by Reynolds' lead citrate and examined in an HT7700 transmission electron microscope (Hitachi High-Tech, Tokyo, Japan) operated at 100 kV. Digital images were acquired using a 2k × 2k Veleta CCD camera (Olympus Soft Imaging Solutions GmbH, Münster, Germany).

2.14. Immunofluorescence Labeling

A549 cells grown on coverslips were fixed by 4% paraformaldehyde (Scharlau, Barcelona, Spain) for 20 min, followed by permeabilization by 0.1% Triton X-100 (VWR) before blocking with 2% bovine serum albumin (BSA) (Fitzgerald, Crossville, TN, USA) and 2% goat serum (Invitrogen) for 1 h. Cells were labeled with the primary antibody anti-LNP (1:250) for 1 h at 37 °C, followed by incubation with the secondary antibody Alexa Fluor 488 (1:1000) under similar conditions. Images were captured using a confocal laser scanning microscopy SP8 (Leica, Germany) and analyzed using ImageJ.

2.15. Statistics

Statistical differences between the means were determined using Student's *t* test or one-way ANOVA followed by Bonferroni post-test, which $p < 0.05$ was considered to indicate a statistically significant difference in the comparison of groups. GraphPad Prism was used for performing all statistical analyses. The values are presented as mean ± standard error of the mean.

3. Results

3.1. LNP Is Essential for WNVKUN, ZIKV, and LGTV Production

The membrane-remodeling protein, LNP plays a role in maintaining the three-way tubular junctions within the ER [16,17], which has highly curve structures like the Ve. Thus,

we sought the effects of the endogenous LNP during flavivirus infection. Initially, LNP depletion in A549 cells was mediated by LNP siRNA transfection. LNP knockdown was demonstrated by immunoblotting of the cell lysates with anti-LNP antibody (Figure 1A).

We infected the LNP knockdown cells and cells transfected with the non-targeting (NT) control siRNA with WNV_{KUN}, ZIKV, or LGTV, followed by determination of the virus titers from the cell culture supernatants, respectively. There were 80–90% reductions of virus titers during LNP depletion compared to the NT control (Figure 1B). Consistently, there were reductions in gene copy numbers of these viruses measured by qPCR during LNP depletion (Figure 1C). During ZIKV infection, we observed around 50% of reduction in gene copy number in comparison with the control, whereas 70-80% of reductions were detected during WNV_{KUN} and LGTV infection, respectively. Collectively, the similar inhibitory trends between virus titers and gene copy numbers suggest the effect of LNP-silencing occurs prior to the virus maturation stage.

To verify the specificity of siRNA silencing, we rescued the virus production phenotype during LNP depletion. As it has been shown that the normal ER structures during LNP removal can be regenerated only by overexpressing certain levels of LNP [23], LNP-depleted cells were transfected with a titer of LNP-mCherry construct, followed by infection with 0.1 MOI of the LGTV. By immunoblotting of cell lysates, there was an increase of the LGTV E protein at high LNP-mCherry-expressing conditions (Figure 1D). Similarly, there was a partial rescue of LGTV production in the supernatant by transfecting cells with a high amount of LNP-mCherry, compared to non-transfection of LNP-mCherry (Figure 1E). Thus, these data suggest a specific role of LNP for LGTV production.

3.2. Requirement of LNP for Intracellular WNV_{KUN}, ZIKV, and LGTV

As we showed that LNP may act prior to virus maturation, we sought to investigate the effects of LNP depletion at earlier stages of the virus life cycle, such as virus assembly and budding. Here, we compared the intracellular infectious particle numbers versus gene copy numbers. siRNA-treated cells were infected with WNV_{KUN}, ZIKV, or LGTV, then harvested and repeatedly frozen/thawed three times in liquid nitrogen to release the intracellular virus particles. In accordance with the virus titers in supernatants, there were significant reductions in titers of infectious intracellular virus particles. Silencing of LNP resulted in 80–90% reductions of virus titers, as measured by plaque assays (Figure 2A). Similarly, virus gene copy numbers from cell lysates were reduced due to LNP depletion. Particularly, LGTV infected cells showed the highest reduction of 80% compared to the negative control. This effect was more moderate in ZIKV and WNV_{KUN} infected cells having reductions by 50–60% (Figure 2B), which indicates an important role of LNP during LGTV infection. Taken together, the similarity between results from plaque assays and qPCR from the cell lysates and supernatants suggests LNP does not act on virus release.

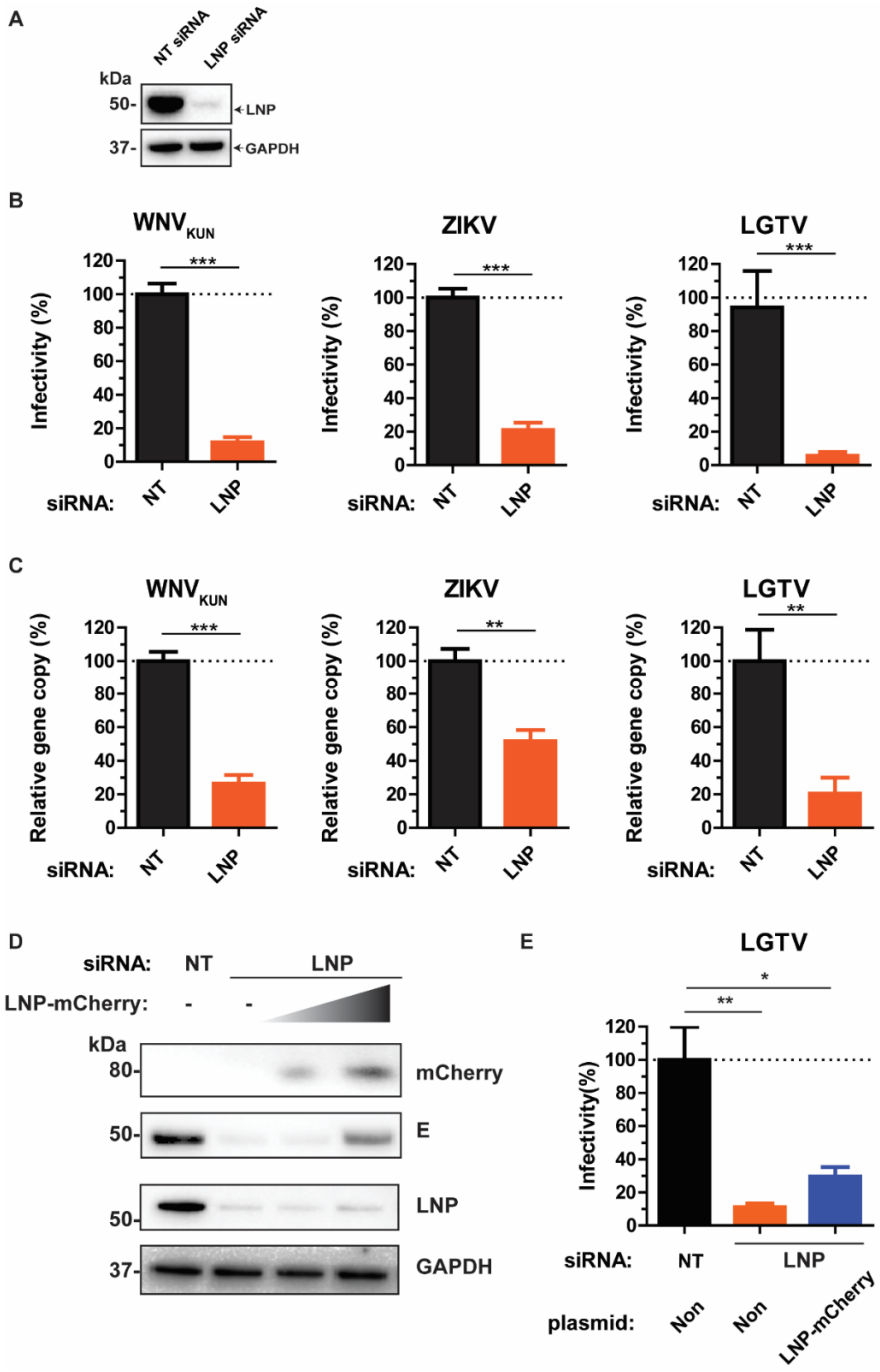

Figure 1. LNP is essential for flavivirus production. (**A**) Immunoblotting of cell lysates 48 h post-transfection with the antibody against LNP after non-targeting (NT) and LNP-targeting siRNA transfection. The expression levels were normalized using the endogenous glyceraldehyde-3-phosphate dehydrogenase (GAPDH) protein as a control. (**B**) The percentages of infectious virus particles released in the supernatants of LNP-silencing cells in comparison with NT-silencing cells after WNV$_{KUN}$, ZIKV, and LGTV virus infections, measured by plaque assays. (**C**) The percentages of gene copy number of viruses released in the supernatants of LNP-silencing cells in comparison with the control, measured by qPCR. (**D**) Immunoblotting of cell lysates after siRNA treatment, transfection with a titer of LNP-mCherry, and infection with 0.1 MOI LGTV. The proteins were visualized with antibodies against mCherry, LNP, LGTV E, and GAPDH as the loading control. (**E**) The percentages of infectious virus particles released in the supernatants of LNP-silencing cells followed by transfection of a high quantity of LNP-mCherry DNA plasmid. The experiments were conducted independently three times with two technical repeats. The p values are indicated using * $p < 0.05$, ** $p < 0.01$, and *** $p < 0.001$.

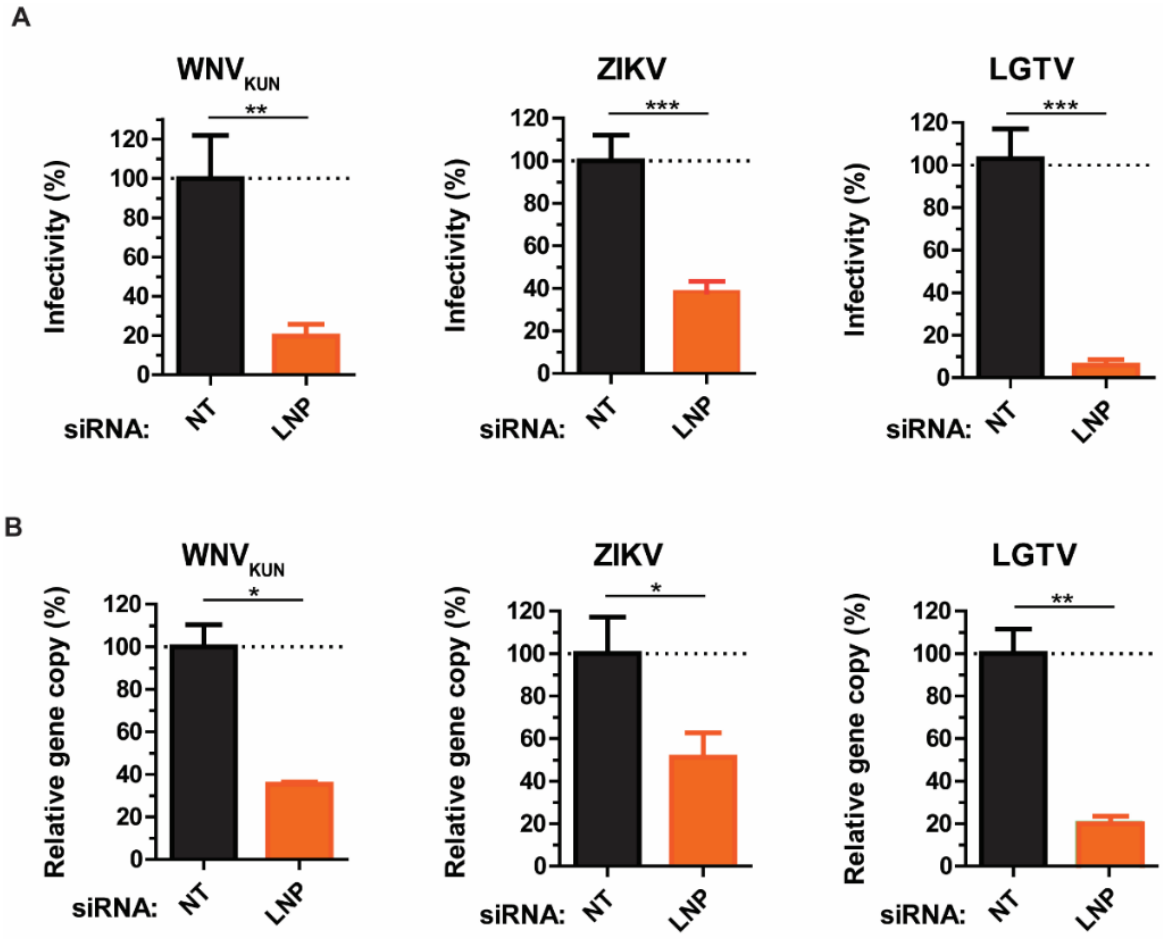

Figure 2. Reductions of intracellular virus titers during LNP depletion. (**A**) The percentages of infectious virus particles in the LNP-silencing cell lysates in comparison with NT controls after WNV_{KUN}, ZIKV, and LGTV infections measured by plaque assays. (**B**) The percentages of virus gene copy numbers measured by qPCR from the LNP-silencing cell lysates in comparison with the controls. The experiments were conducted independently three times with two technical repeats. The *p* values are indicated using * $p < 0.05$, ** $p < 0.01$, and *** $p < 0.001$.

3.3. LNP Has a Role in WNV_{KUN} and LGTV Replication

As our preliminary data suggested that LNP may have an important function during virus replication, we generated cell lines expressing RNA WNV_{KUN} or LGTV replicons, termed BHK-WNV_{KUN} and BHK-LGTV, respectively, to specifically study virus replication. Here, WNV_{KUN} represents a mosquito-borne flavivirus, while the LGTV represents a tick-borne flavivirus. Initially, the RNA replicons were synthesized by in vitro transcription prior to transfection into BHK-21 cells. For replicon synthesis, DNA constructs were created that insert a neomycin/kanamycin resistance (NeoR/KanR) gene, driven by an internal ribosome entry site (IRES), within the 3′-UTR. Resistance to G418 drug killing was conferred to cells expressing the replicon RNA. After selection, the majority of cells expressed the replicating replicons indicated by immunolabeling with dsRNA antibody (Figure 3B). Furthermore, neither BHK-WNV_{KUN} nor BHK-LGTV cells had obvious cytopathic effects compared to the control, as indicated by bright-field images (Figure 3B).

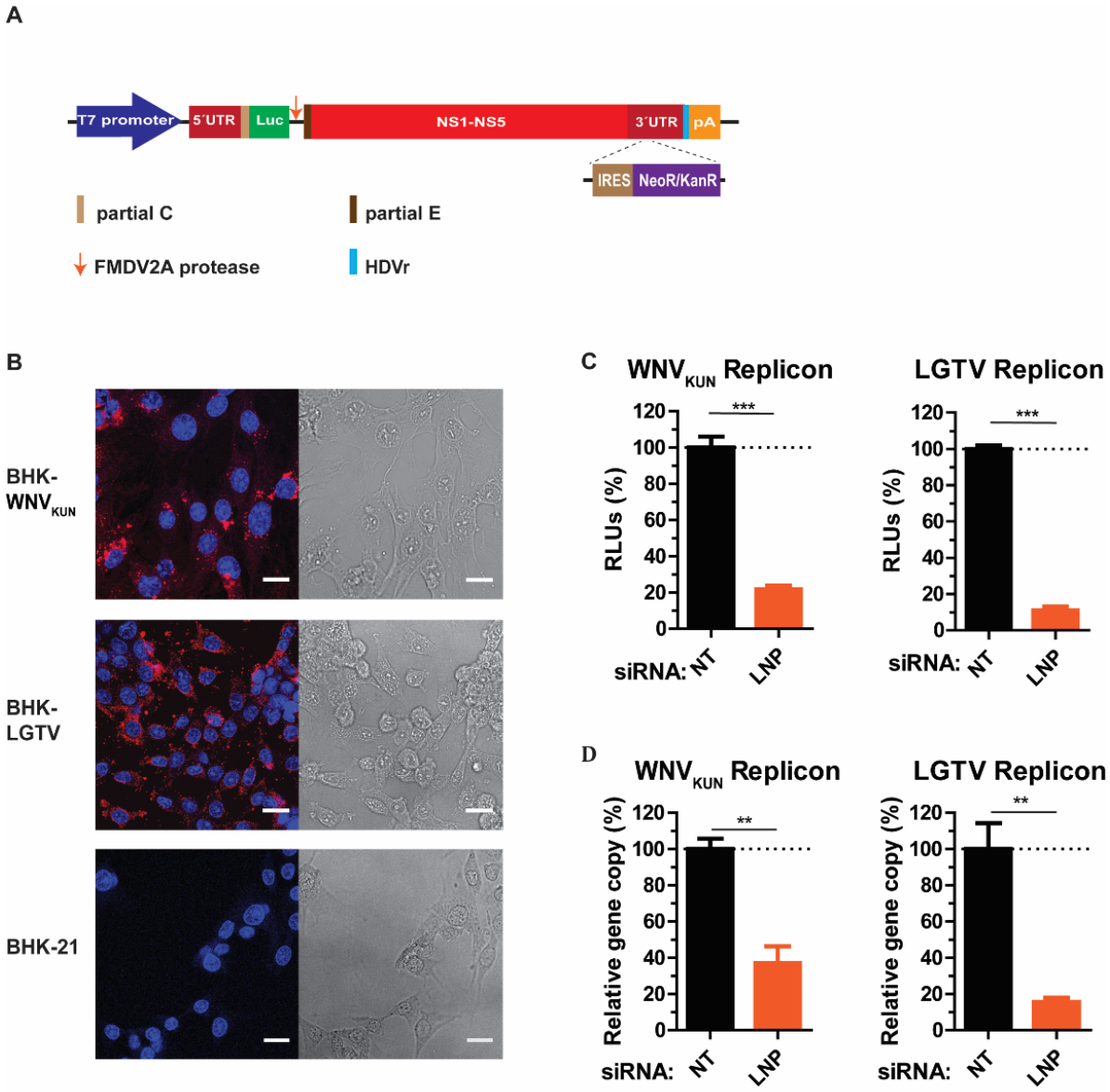

Figure 3. LNP is required for flavivirus replication. (**A**) Schematic illustration of the replicon construct to generate replicon-expressing cell lines. RNA replicons were expressed in vitro by the T7 promotor-driven DNA constructs, which is flanked by the 5′- untranslated region (UTR), the 3′-UTR, and comprises: the firefly luciferase gene (Luc) as a reporter gene in place of genes coding structural proteins, the foot-and-mouth disease virus autoprotease 2a (FMDV 2A), and all the nonstructural proteins of the flavivirus. The antigenomic hepatitis delta virus ribozyme (HDVr) sequence was inserted immediately downstream of the 3′-UTR followed by the simian virus 40 (SV40) polyadenylation signal (pA). An internal ribosome entry site (IRES) sequence and the neomycin/kanamycin resistance (NeoR/KanR) gene were inserted within the 3′-UTR. (**B**) Left panels: Immunofluorescence staining with the dsRNA antibody of the WNV$_{KUN}$ and LGTV replicon-expressing cells. The non-transfected BHK-21 cells were used as the control. The nuclei were counterstained by DAPI (blue). The bar scales represent 20 µm. Right panels: bright field images of the respective cells. (**C**) The percentages of relative luciferase units (RLU) from the BHK-WNV$_{KUN}$ or the BHK-LGTV cell lysates during LNP-silencing in comparison with NT- silencing. (**D**) The percentages of replicon gene copy numbers measured by qPCR from the LNP-silencing cell lysates in comparison with the NT-silencing cell lysates. The experiments were conducted independently three times with two technical repeats. The *p* values are indicated using ** $p < 0.01$, and *** $p < 0.001$.

LNP depletion in BHK-WNV$_{KUN}$ and BHK-LGTV cells resulted in significant reductions of replicon expression, monitored by the activity of the luciferase reporter gene (Figure 3C). There was an 80% and 90% reduction of luciferase expression in LNP-depleted

BHK-WNV_{KUN} and BHK-LGTV cells, respectively. In accordance with the luciferase expression, the replicon gene copy numbers were also reduced by 60% or 80% due to the LNP silencing in BHK-WNV_{KUN} or BHK-LGTV cells, respectively. Altogether, these results suggest that LNP acts during flavivirus replication.

3.4. Function of LNP in Regulating the Number and the Size of Replication Vesicles (Ve)

After we have observed the inhibitory effects on flavivirus replication during LNP silencing, we sought to verify the function of LNP on generation and maintenance of the Ve, assuming it to be the underlying mechanism of reductions in replication. Initially, we analyzed these ER membrane ultrastructures in BHK-WNV_{KUN} cells during LNP depletion compared to the control NT-silencing (Figure 4A). In these cells, the ER membrane is remodeled to generate clusters of Ve, similarly to the duration of the virus infection [6,7], but not in the naïve BHK-21 cells (Figure 4B). We evaluated the number of Ve per cell during LNP silencing versus NT silencing. Interestingly, there was a significant reduction in the numbers of Ve in the LNP-depleted cells compared to the control cells (Figure 4C). Similarly, we observed that there were Ve in the BHK-LGTV cells (Figure 4D) as previously described [24–27]. Interestingly, depletion of LNP resulted in enlargements of the Ve (Figure 4D,E), suggesting defects in the maintenance of the Ve curvature. However, LNP depletion did not alter the number of Ve per cell in the BHK-LGTV cells. Altogether, these results suggest that the reason for reduced replication during LNP depletion is due to the role of LNP in the Ve generation or maintenance.

3.5. LNP Interacts with NS4B

Since we showed that LNP has a function in viral replication and Ve generation, we sought to determine if the protein specifically interacts with viral proteins of the RC. It has been indicated previously that depletion of LNP resulted in a strong inhibitory effect on LGTV, which is the naturally attenuated virus in the TBEV serocomplex [28,29]. To explore LNP interactions with RC components, we first looked for visual recruitment of LNP to viral proteins. We focused our study on the TBEV Europe type NS4A and NS4B proteins that are known to generate Ve [8–10,30]. We expressed a mCherry protein or a mCherry-tagged NS4A-NS4B fusion protein in A549 cells and then immunostained the cells with an anti-LNP antibody (Figure 5A). By measuring the intensity of fluorescent signals representing mCherry versus LNP, we showed that there is close localization between LNP and NS4A-NS4B-mCherry in comparison with the control mCherry (Figure 5A). During the NS4A-NS4B-mCherry expression, we observed fluorescent dots indicative of Ve and the site of LNP recruitment (Figure 5A, upper panel).

As we determined the close localization between NS4A-NS4B-mCherry and LNP at the induced Ve, we sought to investigate if there are direct interactions between these proteins and LNP. We ectopically expressed NS4A, 2K-NS4B, 2K-NS4B TM1–3, 2K-NS4B TM1, or anchored prM-E having the mCherry tag at the protein C-terminus and then immunoprecipitated (IP) mCherry-containing protein complexes from cell lysates with the mCherry antibody (Figure 5B). Here, the anchored prM-E-mCherry acts as a membrane protein control. Furthermore, the 2K domain and the anchored domain of capsid protein in the 2K-NS4B and the anchored prM-E constructs, respectively, allowed the proteins to locate at the ER membrane with correct topologies. During expression, both the 2K and the prM are cleaved from these proteins by host peptidase results in NS4B-mCherry and E-mCherry, respectively [8,31]. LNP co-precipitated from the cell lysates expressing 2K-NS4B-mCherry, but not from NS4A or the other controls (mCherry or prM-E), indicating the interaction between LNP and NS4B (Figure 5B). Interestingly, removal of the TM4 and TM5 of NS4B (Figure 5B,C) aborted the interaction between NS4B and LNP. Overall, the data suggest that LNP is recruited to the RC and that interactions between LNP and the C-terminal region of NS4B is important.

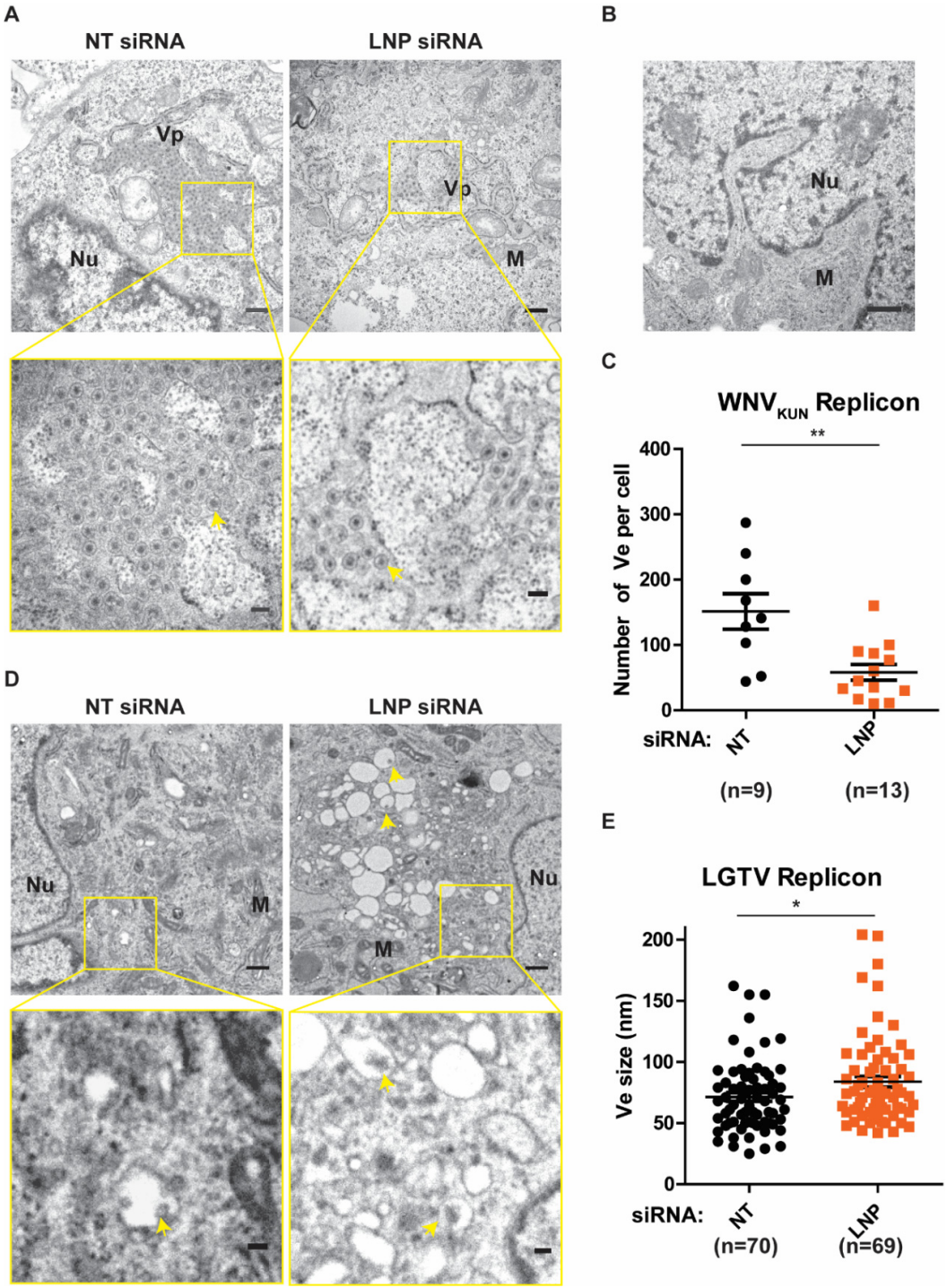

Figure 4. LNP depletion reduced virus-induced vesicles (Ve) in the replicon expressing cell lines. (**A**) Ultrastructural analysis of BHK-WNV$_{KUN}$ cells transfected with NT or LNP siRNA by transmission electron microscopy (TEM). The lower panels show higher magnification images of the yellow boxes indicated in the upper panels, respectively. Scale bars represent 500 nm in the upper panels and 100 nm in the lower panels. Arrows indicate the Ve, ER: the endoplasmic reticulum; Nu: nucleus; M: mitochondria; Vp: vesicle packets. (**B**) TEM image of the BHK-21 cells having no replicons. Scale bar represents 500 nm. (**C**) The number of Ve per WNV$_{KUN}$ cell after LNP deletion compared to the NT silencing control. (**D**) TEM images of BHK-LGTV cells transfected with the indicated siRNA. The lower panels show higher magnification images of the yellow boxes indicated in the upper panels, respectively. Scale bars represent 500 nm in the upper panels and 100 nm in the lower panels. (**E**) The size of Ve in the BHK-LGTV cells. The p values are indicated using * $p < 0.05$ and ** $p < 0.01$.

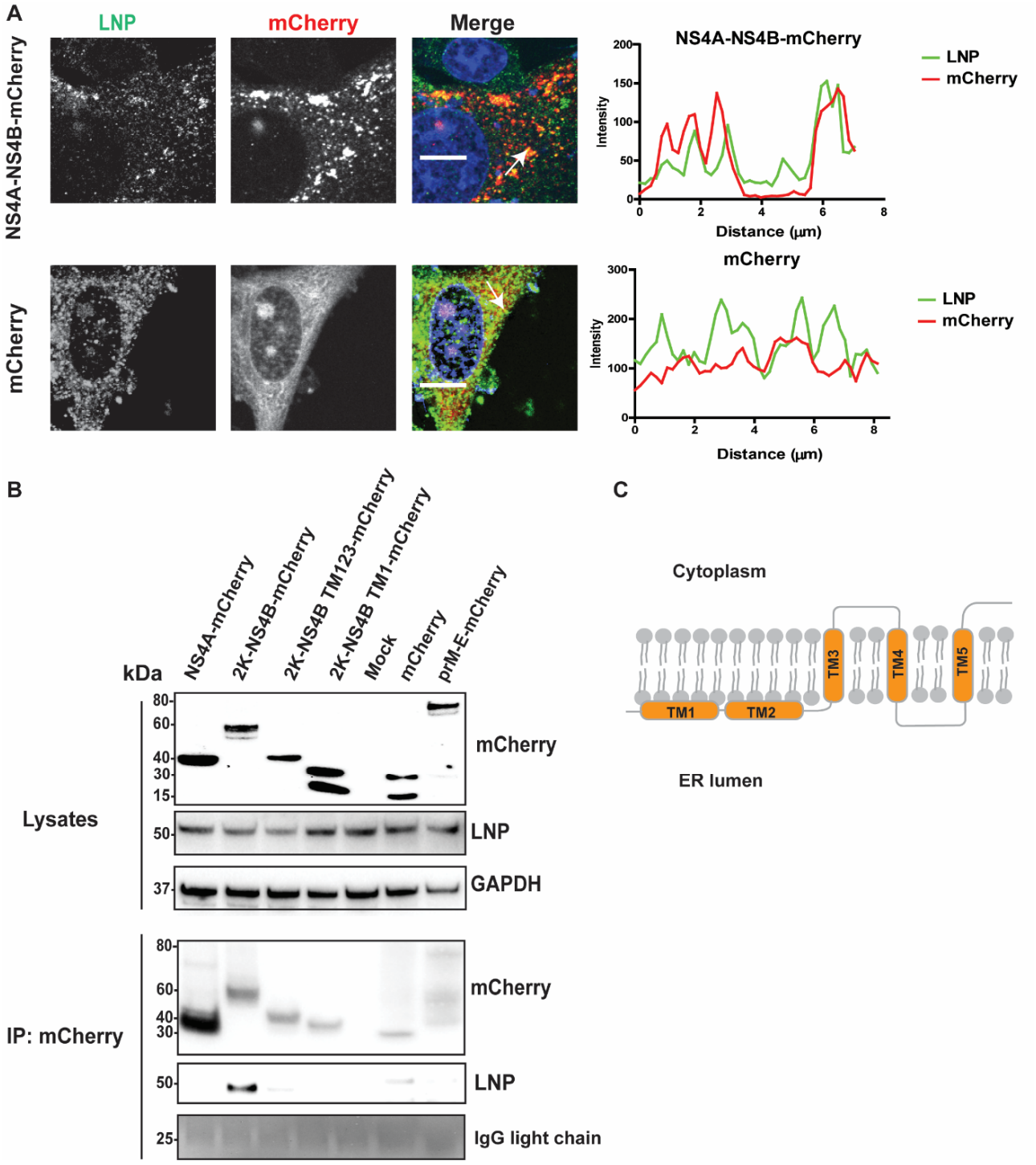

Figure 5. LNP co-localizes and interacts with NS4B. (**A**) Immunofluorescence labeling of cells transfected with NS4A-NS4B-mCherry compared to cells transfected with mCherry. A549 cells were visualized with anti-LNP antibodies (green) and mCherry (red). Nuclei were counterstained with DAPI (blue). Bar scales represent 10 μm. Graphs on the right panel illustrate green and red fluorescent intensity at white arrows in the left images, respectively. (**B**) Immunoblotting of cell lysates 48 h post transfection of the NS4A, 2K-NS4B, 2K-NS4B transmembrane (TM) domain 123, 2K-NS4B TM1, anchored prM-E constructs having the mCherry tag at the protein C-terminal, or the mCherry construct, prior to immunoprecipitation by anti-mCherry beads. The proteins were visualized with antibodies against mCherry, LNP, and GAPDH as the loading control. (**C**) Schema illustrates structure of the polytopic NS4B protein with 5 TM domains spanning the ER membrane.

4. Discussion

Compared to cellular organisms, viruses have a limited genome. During cellular infection, viruses often employ host cell factors for their life cycle and develop mechanisms to delay the host defense system [32,33]. In this study, we attempted to characterize the functions of LNP during the flavivirus life cycle. Initially, we compared the numbers of infectious viral particles with the viral gene copy numbers from the supernatants to evaluate alterations in the viral maturation stage. Then we compared the intracellular and extracellular viral particles to assess changes in virus release. Interestingly, we observed stronger inhibitions during depletions of LGTV compared to WNV_{KUN} and ZIKV, suggesting the preference utility of LNP by tick-borne flaviviruses.

In addition, we generated cell lines expressing the WNV_{KUN} or LGTV replicons, which represent mosquito-borne and tick-borne flaviviruses, respectively, to specifically study viral replication. Our replicon platforms did not show major cytopathic effects and maintained the replicon expression for many passages (data not shown), which is similar to a previously described system [34]. We showed that insertion of the IRES-NeoR/KanR in a variant region of the 3′UTR did not abolish the replication capacity of the replicons but conferred an antibiotic resistance capacity to transfected cells. These cell lines can be good systems to study proteins of the host machinery having roles in the virus replication such as LNP in our study and can be platforms for screening antiviral-compounds targeting the virus replication.

In this study, we showed that LNP depletion resulted in defective replication of WNV_{KUN} and LGTV. These inhibitory effects were due to the role of LNP in either induction or stabilization of the Ve. Interestingly, the protein interacts specifically with NS4B that is a TM protein scaffolding the RC. The protein is linked to NS4A by the 2K domain that is initially cleaved by NS2B/NS3 to form 2K-NS4B [8], followed by the host signal peptidase SPCS1-mediated cleavage to remove the 2K [8,35]. NS4B is a conserved protein in flaviviruses with five integral TM domains (Figure 5C), mutations of which abrogate virus replication and decrease virulence [36]. The protein contains multiple interaction motifs for dimerization, interaction with other NS proteins in the RC and host proteins [36]. In our study, we found that the C-terminal region of NS4B containing the TM4-5 may be essential for the interaction of the protein with LNP.

In eukaryotic cells, the ER is a dynamic constant-remodeling membranous organelle spreading throughout the cytoplasm [37]. This network consists of sheets and tubules interconnected by three-way junctions. The conserved membrane protein LNP localizes at the ER junctions and stabilizes them [17], as depletions of the protein have resulted in a densely sheet-like ER [16,23,38]. The ER phenotype can be rescued by overexpression of LNP at a certain level [23]. In our study, we partially rescued the LGTV production by overexpressing LNP from the LNP-mCherry construct. We speculate that higher virus production can be rescued by using other LNP construct having codons optimized to resist siRNA or by higher overexpression of LNP construct in cell lines stably depleting LNP.

Furthermore, the LNP protein has been shown to be ubiquitinated and recruit the rapamycin complex-1 at the ER three-way junction and lysosomes. Inhibition of LNP ubiquitination triggers neurodevelopmental defects [39]. In this study, we propose a role of LNP during flavivirus replication as the protein is recruited to the Ve, mainly located at the ER [40], by its interaction with NS4B. However, the question that the LNP-NS4B interaction can hinder the LNP ubiquitination, resulting in the neural cytopathic effects during flavivirus infections, remains for future studies.

Other ER three-way junctions inducers and stabilizers have also been characterized during flavivirus infection including RTN [41,42], DP1 [12,13], and ATL [14,15]. Indeed, RTN3 has been shown to act in the formation of the Ve for WNV_{KUN}, Dengue virus serotype 2 (DENV-2), and ZIKV, by interacting with NS4A [18]. In that study, depletions of RTN3 significantly inhibited the intracellular gene copy number of ZIKV but was less effective with DENV-2 and WNV_{KUN} [18]. In addition to flaviviruses, this protein is also employed for the replication of other RNA viruses, including enterovirus A71 [43], brome

mosaic virus, and hepatitis C virus [44]. Furthermore, silencing of SEC61β that interacts with RTN1 [45] resulted in a reduction of WNV_{KUN} and DENV-2 production [35]. In addition to the RTN family, the endogenous ATL2 [19] has been shown to function in replication and formation of the Ve in DENV-2 and ZIKV but not WNV (strain NY99) [19] by its interaction with NS3. Contradictory, LNP and RTN3 appeared to have no effect on DENV-2 from the study [19]. In our study, we have shown that LNP plays a role in Ve formation and replication for two neurotropic flaviviruses, WNV_{KUN} and LGTV. We also demonstrated that the protein interacts with NS4B and that TM4–5 may have a direct role in the interaction. Therefore, these observations indicate the divergence of flaviviruses in employing the orchestra of ER-shaping proteins: LNP, RTN, and ATL for Ve generation. Interestingly, LNP has been demonstrated to act in synergy with RTN but antagonism to ATL to remodel the ER [16,38], which suggests enhanced anti-flavivirus conditions for future investigations.

5. Conclusions

In conclusion, this study has contributed new understandings of the role of host proteins during flavivirus replication. Our results suggested that LNP is important for the Ve formation during the replication of the mosquito-borne WNV_{KUN} and the tick-borne LGTV using the established replicon-expressing cell lines. LNP has also been shown to interact with the C-terminus of NS4B.

Author Contributions: Conceptualization, P.-T.-H.T., M.J. and W.M.; methodology, P.-T.-H.T., N.A. and W.M.; software, P.-T.-H.T.; formal analysis, P.-T.-H.T.; writing—original draft preparation, P.-T.-H.T.; writing—review and editing, P.-T.-H.T., N.A., M.J. and W.M.; visualization, P.-T.-H.T.; supervision, M.J. and W.M.; project administration, M.J. and W.M.; funding acquisition, M.J. All authors have read and agreed to the published version of the manuscript.

Funding: This research was funded by grants to M.J. by the Knowledge Foundation (20190091 and 20200063). The funding body played no role in the design of the study and collection, analysis, interpretation of data, and in writing the manuscript.

Institutional Review Board Statement: Not applicable.

Informed Consent Statement: Not applicable.

Data Availability Statement: The data presented in this study is available in this article. Remaining data supporting reported results is available from the corresponding authors upon reasonable requests.

Acknowledgments: We thank Lars Haag (Department of Laboratory Medicine, Karolinska Institute, Stockholm, Sweden) for excellent technical assistance in electron microscopy. We also thank Travis Taylor (Department of Medical Microbiology and Immunology, University of Toledo, Toledo, OH, USA) for valuable comments on the manuscript.

Conflicts of Interest: The authors declare no conflict of interest.

References

1. Calisher, C.H.; Karabatsos, N.; Dalrymple, J.M.; Shope, R.E.; Porterfield, J.S.; Westaway, E.G.; Brandt, W.E. Antigenic Relationships between Flaviviruses as Determined by Cross-neutralization Tests with Polyclonal Antisera. *J. Gen. Virol.* **1989**, *70*, 37–43. [CrossRef]
2. Krauer, F.; Riesen, M.; Reveiz, L.; Oladapo, O.T.; Martínez-Vega, R.; Porgo, T.V.; Haefliger, A.; Broutet, N.J.; Low, N.; WHO Zika Causality Working Group. Zika virus infection as a cause of congenital brain abnormalities and Guillain–Barré syndrome: Systematic review. *PLoS Med.* **2017**, *14*, e1002203. [CrossRef]
3. Gritsun, T.S.; Lashkevich, V.A.; Gould, E.A. Tick-borne encephalitis. *Antivir. Res.* **2003**, *57*, 129–146. [CrossRef]
4. Mandl, C.W. Steps of the tick-borne encephalitis virus replication cycle that affect neuropathogenesis. *Virus Res.* **2005**, *111*, 161–174. [CrossRef]
5. Apte-Sengupta, S.; Sirohi, D.; Kuhn, R.J. Coupling of replication and assembly in flaviviruses. *Curr. Opin. Virol.* **2014**, *9*, 134–142. [CrossRef]
6. Mackenzie, J.M.; Jones, M.K.; Westaway, E.G. Markers for trans-Golgi membranes and the intermediate compartment localize to induced membranes with distinct replication functions in flavivirus-infected cells. *J. Virol.* **1999**, *73*, 9555–9567. [CrossRef]

7. Westaway, E.G.; Mackenzie, J.M.; Kenney, M.T.; Jones, M.K.; Khromykh, A.A. Ultrastructure of Kunjin virus-infected cells: Colocalization of NS1 and NS3 with double-stranded RNA, and of NS2B with NS3, in virus-induced membrane structures. *J. Virol.* **1997**, *71*, 6650–6661. [CrossRef]
8. Roosendaal, J.; Westaway, E.G.; Khromykh, A.; Mackenzie, J.M. Regulated cleavages at the West Nile virus NS4A-2K-NS4B junctions play a major role in rearranging cytoplasmic membranes and Golgi trafficking of the NS4A protein. *J. Virol.* **2006**, *80*, 4623–4632. [CrossRef]
9. Kaufusi, P.H.; Kelley, J.F.; Yanagihara, R.; Nerurkar, V.R. Induction of endoplasmic reticulum-derived replication-competent membrane structures by West Nile virus non-structural protein 4B. *PLoS ONE* **2014**, *9*, e84040. [CrossRef]
10. Miller, S.; Kastner, S.; Krijnse-Locker, J.; Bühler, S.; Bartenschlager, R. The non-structural protein 4A of dengue virus is an integral membrane protein inducing membrane alterations in a 2K-regulated manner. *J. Biol. Chem.* **2007**, *282*, 8873–8882. [CrossRef]
11. English, A.R.; Voeltz, G.K. Endoplasmic reticulum structure and interconnections with other organelles. *Cold Spring Harb. Perspect. Biol.* **2013**, *5*, a013227. [CrossRef]
12. Shibata, Y.; Voss, C.; Rist, J.M.; Hu, J.; Rapoport, T.A.; Prinz, W.A.; Voeltz, G.K. The reticulon and DP1/Yop1p proteins form immobile oligomers in the tubular endoplasmic reticulum. *J. Biol. Chem.* **2008**, *283*, 18892–18904. [CrossRef]
13. Hu, J.; Shibata, Y.; Voss, C.; Shemesh, T.; Li, Z.; Coughlin, M.; Kozlov, M.M.; Rapoport, T.A.; Prinz, W.A. Membrane Proteins of the Endoplasmic Reticulum Induce High-Curvature Tubules. *Science* **2008**, *319*, 1247. [CrossRef]
14. Hu, J.; Shibata, Y.; Zhu, P.-P.; Voss, C.; Rismanchi, N.; Prinz, W.A.; Rapoport, T.A.; Blackstone, C. A Class of Dynamin-like GTPases Involved in the Generation of the Tubular ER Network. *Cell* **2009**, *138*, 549–561. [CrossRef]
15. Anwar, K.; Klemm, R.W.; Condon, A.; Severin, K.N.; Zhang, M.; Ghirlando, R.; Hu, J.; Rapoport, T.A.; Prinz, W.A. The dynamin-like GTPase Sey1p mediates homotypic ER fusion in S. *cerevisiae*. *J. Cell Biol.* **2012**, *197*, 209–217. [CrossRef]
16. Chen, S.; Novick, P.; Ferro-Novick, S. ER network formation requires a balance of the dynamin-like GTPase Sey1p and the Lunapark family member Lnp1p. *Nat. Cell Biol.* **2012**, *14*, 707–716. [CrossRef]
17. Chen, S.; Desai, T.; McNew, J.A.; Gerard, P.; Novick, P.J.; Ferro-Novick, S. Lunapark stabilizes nascent three-way junctions in the endoplasmic reticulum. *Proc. Natl. Acad. Sci. USA* **2015**, *112*, 418–423. [CrossRef]
18. Aktepe, T.E.; Liebscher, S.; Prier, J.E.; Simmons, C.P.; Mackenzie, J.M. The Host Protein Reticulon 3.1A Is Utilized by Flaviviruses to Facilitate Membrane Remodelling. *Cell Rep.* **2017**, *21*, 1639–1654. [CrossRef]
19. Neufeldt, C.J.; Cortese, M.; Scaturro, P.; Cerikan, B.; Wideman, J.G.; Tabata, K.; Moraes, T.; Oleksiuk, O.; Pichlmair, A.; Bartenschlager, R. ER-shaping atlastin proteins act as central hubs to promote flavivirus replication and virion assembly. *Nat. Microbiol.* **2019**, *4*, 2416–2429. [CrossRef]
20. Monel, B.; Rajah, M.M.; Hafirassou, M.L.; Sid Ahmed, S.; Burlaud-Gaillard, J.; Zhu, P.P.; Nevers, Q.; Buchrieser, J.; Porrot, F.; Meunier, C.; et al. Atlastin Endoplasmic Reticulum-Shaping Proteins Facilitate Zika Virus Replication. *J. Virol.* **2019**, *93*. [CrossRef]
21. Smith, C.E. A virus resembling Russian spring-summer encephalitis virus from an ixodid tick in Malaya. *Nature* **1956**, *178*, 581–582. [CrossRef]
22. Tran, P.T.; Asghar, N.; Höglund, U.; Larsson, O.; Haag, L.; Mirazimi, A.; Johansson, M.; Melik, W. Development of a Multivalent Kunjin Virus Reporter Virus-Like Particle System Inducing Seroconversion for Ebola and West Nile Virus Proteins in Mice. *Microorganisms* **2020**, *8*, 1890. [CrossRef]
23. Asghar, N.; Lee, Y.P.; Nilsson, E.; Lindqvist, R.; Melik, W.; Kröger, A.; Överby, A.K.; Johansson, M. The role of the poly(A) tract in the replication and virulence of tick-borne encephalitis virus. *Sci. Rep.* **2016**, *6*, 39265. [CrossRef]
24. Wang, S.; Tukachinsky, H.; Romano, F.B.; Rapoport, T.A. Cooperation of the ER-shaping proteins atlastin, lunapark, and reticulons to generate a tubular membrane network. *Elife* **2016**, *5*. [CrossRef] [PubMed]
25. Bílý, T.; Palus, M.; Eyer, L.; Elsterová, J.; Vancová, M.; Růžek, D. Electron Tomography Analysis of Tick-Borne Encephalitis Virus Infection in Human Neurons. *Sci. Rep.* **2015**, *5*, 10745. [CrossRef] [PubMed]
26. Offerdahl, D.K.; Dorward, D.W.; Hansen, B.T.; Bloom, M.E. A Three-Dimensional Comparison of Tick-Borne Flavivirus Infection in Mammalian and Tick Cell Lines. *PLoS ONE* **2012**, *7*, e47912. [CrossRef] [PubMed]
27. Miorin, L.; Romero-Brey, I.; Maiuri, P.; Hoppe, S.; Krijnse-Locker, J.; Bartenschlager, R.; Marcello, A. Three-Dimensional Architecture of Tick-Borne Encephalitis Virus Replication Sites and Trafficking of the Replicated RNA. *J. Virol.* **2013**, *87*, 6469–6481. [CrossRef] [PubMed]
28. Yau, W.-L.; Nguyen-Dinh, V.; Larsson, E.; Lindqvist, R.; Överby, A.K.; Lundmark, R. Model System for the Formation of Tick-Borne Encephalitis Virus Replication Compartments without Viral RNA Replication. *J. Virol.* **2019**, *93*, e00292-19. [CrossRef]
29. Rumyantsev, A.A.; Murphy, B.R.; Pletnev, A.G. A tick-borne Langat virus mutant that is temperature sensitive and host range restricted in neuroblastoma cells and lacks neuroinvasiveness for immunodeficient mice. *J. Virol.* **2006**, *80*, 1427–1439. [CrossRef] [PubMed]
30. Miller, S.; Sparacio, S.; Bartenschlager, R. Subcellular localization and membrane topology of the Dengue virus type 2 Non-structural protein 4B. *J. Biol. Chem.* **2006**, *281*, 8854–8863. [CrossRef]
31. Markoff, L.; Chang, A.; Falgout, B. Processing of flavivirus structural glycoproteins: Stable membrane insertion of premembrane requires the envelope signal peptide. *Virology* **1994**, *204*, 526–540. [CrossRef]
32. Chen, S.; Wu, Z.; Wang, M.; Cheng, A. Innate Immune Evasion Mediated by Flaviviridae Non-Structural Proteins. *Viruses* **2017**, *9*, 291. [CrossRef]

33. Suthar, M.S.; Aguirre, S.; Fernandez-Sesma, A. Innate immune sensing of flaviviruses. *PLoS Pathog.* **2013**, *9*, e1003541. [CrossRef] [PubMed]
34. Khromykh, A.A.; Westaway, E.G. Subgenomic replicons of the flavivirus Kunjin: Construction and applications. *J. Virol.* **1997**, *71*, 1497–1505. [CrossRef]
35. Zhang, R.; Miner, J.J.; Gorman, M.J.; Rausch, K.; Ramage, H.; White, J.P.; Zuiani, A.; Zhang, P.; Fernandez, E.; Zhang, Q.; et al. A CRISPR screen defines a signal peptide processing pathway required by flaviviruses. *Nature* **2016**, *535*, 164–168. [CrossRef] [PubMed]
36. Zmurko, J.; Neyts, J.; Dallmeier, K. Flaviviral NS4b, chameleon and jack-in-the-box roles in viral replication and pathogenesis, and a molecular target for antiviral intervention. *Rev. Med. Virol.* **2015**, *25*, 205–223. [CrossRef]
37. Lee, C.; Chen, L.B. Dynamic behavior of endoplasmic reticulum in living cells. *Cell* **1988**, *54*, 37–46. [CrossRef]
38. Sun, J.; Movahed, N.; Zheng, H. LUNAPARK Is an E3 Ligase That Mediates Degradation of ROOT HAIR DEFECTIVE3 to Maintain a Tubular ER Network in Arabidopsis. *Plant Cell* **2020**, *32*, 2964. [CrossRef]
39. Yuniati, L.; Lauriola, A.; Gerritsen, M.; Abreu, S.; Ni, E.; Tesoriero, C.; Onireti, J.O.; Low, T.Y.; Heck, A.J.R.; Vettori, A.; et al. Ubiquitylation of the ER-Shaping Protein Lunapark via the CRL3(KLHL12) Ubiquitin Ligase Complex. *Cell Rep.* **2020**, *31*, 107664. [CrossRef]
40. Mackenzie, J.M.; Westaway, E.G. Assembly and maturation of the flavivirus Kunjin virus appear to occur in the rough endoplasmic reticulum and along the secretory pathway, respectively. *J. Virol.* **2001**, *75*, 10787–10799. [CrossRef]
41. Voeltz, G.K.; Prinz, W.A.; Shibata, Y.; Rist, J.M.; Rapoport, T.A. A class of membrane proteins shaping the tubular endoplasmic reticulum. *Cell* **2006**, *124*, 573–586. [CrossRef] [PubMed]
42. De Craene, J.O.; Coleman, J.; Estrada de Martin, P.; Pypaert, M.; Anderson, S.; Yates, J.R., 3rd; Ferro-Novick, S.; Novick, P. Rtn1p is involved in structuring the cortical endoplasmic reticulum. *Mol. Biol. Cell* **2006**, *17*, 3009–3020. [CrossRef] [PubMed]
43. Tang, W.F.; Yang, S.Y.; Wu, B.W.; Jheng, J.R.; Chen, Y.L.; Shih, C.H.; Lin, K.H.; Lai, H.C.; Tang, P.; Horng, J.T. Reticulon 3 binds the 2C protein of enterovirus 71 and is required for viral replication. *J. Biol. Chem.* **2007**, *282*, 5888–5898. [CrossRef]
44. Wu, M.-J.; Ke, P.-Y.; Hsu, J.T.A.; Yeh, C.-T.; Horng, J.-T. Reticulon 3 interacts with NS4B of the hepatitis C virus and negatively regulates viral replication by disrupting NS4B self-interaction. *Cell. Microbiol.* **2014**, *16*, 1603–1618. [CrossRef] [PubMed]
45. Zhao, X.; Jäntti, J. Functional characterization of the trans-membrane domain interactions of the Sec61 protein translocation complex beta-subunit. *BMC Cell Biol.* **2009**, *10*, 76. [CrossRef]